200 km Fiber-Loop Conventional Brillouin Distributed Sensor with 2m Spatial Resolution Using Image Denoising

Marcelo A. Soto, Jaime A. Ramírez, Luc Thévenaz
EPFL Swiss Federal Institute of Technology, Institute of Electrical Engineering, SCI STI LT, Station 11, CH-1015 Lausanne, Switzerland
Author e-mail address: marcelo.soto@epfl.ch

Abstract: Non-local means image denoising method is optimized to boost the performance of Brillouin distributed fiber sensors. Results demonstrate ultra-long sensing over a 200-km fiber-loop with 2m resolution using a sensing scheme without any hardware sophistication.
OCIS codes: (060.2310) Fiber optics; (060.2370) Fiber optics sensors; (290.5900) Scattering, stimulated Brillouin; (060.4370) Nonlinear optics, fibers; (100.2000) Digital image processing.

1. Introduction

Brillouin distributed optical fiber sensors have competitive advantages compared to other distributed sensing methods, especially when aiming at very long sensing ranges. The time-domain interrogation approach based on a pump-probe interaction, named Brillouin optical time-domain analysis (BOTDA) [1], has enabled distributed sensing over several tens of kilometers with spatial resolutions typically of a few meters [2]. After more than two decades of research, the factors ultimately limiting the performance of BOTDA sensors have been clearly identified. Among different factors, the measurement signal-to-noise ratio (SNR) is the parameter of uttermost importance defining the sensor performance [2,3]. Unfortunately, the maximum pump and probe powers that can be launched into the fiber are limited by the onset of nonlinear effects, such as modulation instability (MI) [4] and amplified spontaneous Brillouin scattering [5].

Several techniques have been proposed in the state-of-the-art to improve the performance of BOTDA systems and to make them more robust against detrimental effects: optical pulse coding [6] and distributed Raman amplification [7] have allowed enhancing the measurement SNR, while maintaining the peak pump power below the onset of MI. However, such methods require some modifications of the conventional BOTDA scheme, which in some cases can lead to complex configurations, mainly when combining several techniques in a single system [8,9]. Recently a software method based on image processing has been proposed [10,11] to enhance the performance of distributed fiber sensors. State-of-the-art results have shown that the SNR can be considerably enhanced by image denoising, obtaining similar or even better performance when compared to other techniques for performance enhancement.

In this paper, a specific image denoising method, called non-local means (NLM), is optimized to extend the sensing range of a conventional BOTDA sensor. The impact of the denoising parameters is described in order to ensure a significant SNR enhancement with no loss of information. To the best of our knowledge, results represent the first demonstration of a conventional BOTDA sensor (i.e. with no modification on the standard scheme) enabling a 100 km sensing range, in a 200 km fiber-loop, with 2 m spatial resolution and a standard acquisition time of a few minutes.

2. Optimizing NLM denoising for ultra-long range BOTDA sensor

The idea exploited here is based on the high level of redundancy of information contained in the data measured by BOTDA sensors [10,11]. This means that the 2D data structure containing the measured Brillouin gain response at each fiber location z for different pump-probe frequency offsets Δf contains repeated structures that can be efficiently used to reduce noise. In particular, the Brillouin gain associated to each sampled point in the spatio-frequency domain $(z, \Delta f)$ can be processed by an image denoising procedure associating the measured gain value to the intensity of a gray (or monochromatic) image corrupted by noise. Previous results have demonstrated the benefits of using image denoising methods in BOTDA sensors [10,11]. This work however focuses on the optimization of a specific denoising method, so-called non-local means [12], for ultra-long-range BOTDA sensing, aiming at a 200 km fiber-loop. This means that the optimization here is performed under a much more demanding SNR condition, thus testing the ultimate denoising capabilities of the NLM for BOTDA sensing enhancement.

The NLM method [12] applies a weighted averaging strategy to eliminate noise using weighting factors that depends on the similarity of the data existing in the spatio-frequency domain $(z, \Delta f)$ of the measurements. The method requires finding 3 parameters [10-12]: size of the *similarity windows* (2D windows that are compared over the entire or a partial set of data); size of the *searching window* (2D regions where similarity windows are compared), and a *smoothing parameter* h, which controls the weighting factors depending on the noise of the data.

It is worth mentioning that in a 200 km fiber-loop BOTDA system, the probe power is attenuated up to 40 dB by the intrinsic fiber loss. To detect the low-power signal reaching the photo-receiver, a low-noise optical amplifier is usually placed at the receiver front-end, making BOTDA measurements highly dominated by amplified spontaneous emission (ASE) [3]. Since the measured time-domain traces are essentially made of a strong DC probe component, topped by a very small Brillouin amplification (about 1%), the Brillouin response has negligible contribution to the total noise of the system [3]. Thus, the dominating ASE-signal beat noise can be considered to be independent of the longitudinal evolution of the sensor response, so totally constant and stationary. This condition is actually ideal for NLM denoising, making the method an efficient tool to reduce noise in long-range BOTDA sensors.

3. Experimental results

In order to evaluate the use of NLM denoising for ultra-long range sensing, a conventional BOTDA scheme has been implemented with no additional sophistications (e.g. see Fig. 1 in [10] for details on a standard BOTDA setup). Time-domain BOTDA traces have been acquired with 2k averages per scanned frequency, while 300 frequencies have been scanned with steps of 1 MHz. The acquired data have been arrayed in a 2D matrix $M(z, \Delta f)$, containing the Brillouin gain response for the different pump-probe frequency offsets Δf at each longitudinal point z sampled every 0.5 m along the fiber. This has led to a matrix $M(z, \Delta f)$ of very large size: 200'000x300.

The NLM optimization is here performed following a basic procedure [12]. First, the smoothing parameter h is set to 10 times the noise standard deviation σ, where σ is measured to be 0.0114% of the detected probe. To optimize the similarity window it should be considered that the longitudinal sampling interval of the measurements is 0.5 m/pt and the spatial resolution is 2 m. Only a window size of $3x3$ is found to secure no data over-smoothing over fiber sections longer than the spatial resolution (4 points). Then, the searching window size is empirically optimized by testing window dimensions ranging from $7x7$ up to $19x19$. Our exhaustive search indicates that reducing too much the searching area results in a low number of similar patterns found by the processing, leading to non-optimized SNR. However, for very large searching windows, the processing time turned out to be extremely long, while some loss in the spatial resolution could be observed. Actually it has been experimentally verified that using similarity windows of $3x3$ and $h = 1.14\cdot10^{-3}$, a satisfactory amount of noise is removed with a searching window of $13x13$. Increasing this searching area only leads to a marginal SNR improvement at the cost of much longer processing times.

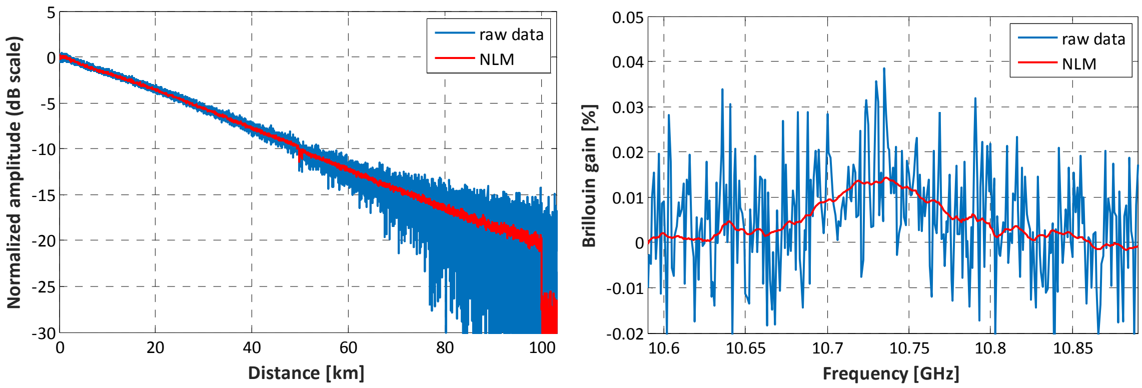

Fig. 1. (a) BOTDA trace at the peak Brillouin gain frequency, and (b) Brillouin gain spectrum measured near the farthest end of the sensing range (i.e. near 100 km distance), obtained from the raw (blue lines) and denoised (red lines) data.

Fig. 1(a) shows traces at the peak Brillouin gain frequency obtained from the raw (blue) and denoised (red) data. The large amount of removed noise and significant increase in the trace contrast are evident in the figure. It turns out that an SNR improvement of 12.5 dB could be verified in this case. Note that the SNR improvement here is lower than the amount reported in [10]; however, it should be mentioned that the SNR on the raw data is practically 0 dB at the end of the 100 km range (after 42 dB of probe attenuation), making the signal presence extremely tenuous. Interestingly the NLM could recover the gain response in this case. It was experimentally verified that this SNR of 0 dB can be considered as the lowest SNR in the system to reliably restore the data contained in the measurements. This could be explained by the fact that larger amount of noise, leading to negative SNR values (in dB scale), would dominate over the real data, preventing image processing from performing a reliable denoising. Fig. 1(b) shows the Brillouin gain spectrum at 100 km distance for the raw and denoised data. This figure highlights the benefits of image denoising to recover the gain response contained in the noisy measurement, even under this very low SNR condition.

By fitting a parabolic curve over the denoised gain spectrum at each fiber location [2], the distributed profile of the Brillouin frequency shift (BFS) has been retrieved. To evaluate the frequency uncertainty, the standard deviation of the BFS retrieved after denoising has been calculated at each fiber location, as shown in Fig. 2(a). The red dashed line represents the exponential fitting of the calculated uncertainty as a function of distance, verifying a frequency uncertainty of 0.77 MHz at 100 km. Finally, Fig. 2(b) shows a 2 m-long hot-spot detection, obtained by heating 2 m of fiber, near 100 km distance, raised 20 K above the ambient temperature. The figure demonstrates that the optimized NLM denoising does not distort the data and no loss of information occurs, correctly resolving a spot event.

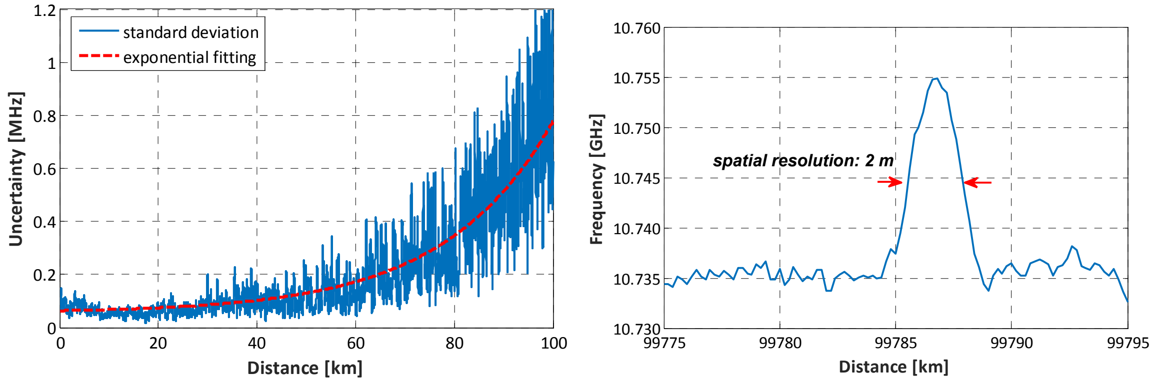

Fig. 2. (a) Frequency uncertainty on the BFS along the 100 km sensing range, obtained from the denoised data of repeated measurements. (b) Demonstration of a 2 m-long hot-spot detection near the farthest end of the sensing range when using NLM.

It should be pointed out that the hot-spot measurement plays a key role in the optimization, showing the actual spatial capabilities of the sensor. Thus, during the evaluation of different searching window sizes, the effect on the hot-spot value has been evaluated. The searching window size of $13x13$ was found to be the optimal size ensuring the highest possible SNR and no distortion of the hot-spot measurement. Searching windows larger than $13x13$ have blurred the information contained in the 2D data, leading to a loss of contrast in the retrieved hot-spot value, inducing errors of 1.8 MHz and 3.2 MHz for sizes of $17x17$ and $19x19$, respectively. Once the optimal searching window size has been identified, the impact of the smoothing parameter h has been evaluated. By changing h from 5σ up to 30σ, the optimal value has been found to be $h \approx 10\sigma$, similar to the originally set value. Results confirm that the use of optimized smoothing parameter and searching window is essential to provide a reliable denoising of the BOTDA data.

In conclusion, by optimizing an image denoising method based on NLM, a sensing range of 100 km in a 200 km fiber-loop has been experimentally demonstrated with 2 m spatial resolution using a standard BOTDA scheme. To the best of our knowledge, this is the first time that a plain BOTDA scheme over such a distance is demonstrated with no hardware modifications. The performance is rated by a figure-of-merit (FoM) [2] equal to 225'000, which corresponds to the highest FoM demonstrated using a standard BOTDA sensor. It is anticipated that image denoising combined with other techniques for BOTDA enhancement, such as pulse coding and/or Raman amplification, can lead to a noticeably increased performance, rated by a much larger FoM.

The authors acknowledge the support from the Swiss Commission for Technology and Innovation (Project 18337.2 PFNM-NM) and are thankful to Omnisens SA for their active discussions and interest in this research.

4. References

[1] T. Horiguchi, *et al*, "Development of a distributed sensing technique using Brillouin scattering," J. Lightw. Technol. **13**(7), 1296-1302 (1995).
[2] M. A. Soto and L. Thévenaz, "Modeling and evaluating the performance of Brillouin distributed optical fiber sensors," Opt. Express **21**(25), 31347–31366 (2013).
[3] M. A. Soto and L. Thévenaz, "Towards 1'000'000 resolved points in a distributed optical fibre sensor." Proc. SPIE **9157**, 9157C3 (2014).
[4] M. Alem, M. A. Soto, and L. Thévenaz, "Analytical model and experimental verification of the critical power for modulation instability in optical fibers," Opt. Express **23**(23), 29514-29532 (2015).
[5] L. Thévenaz, *et al*, "Effect of pulse depletion in a Brillouin optical time-domain analysis system," Opt. Express **21**(12), 14017–14035 (2013).
[6] M. A. Soto, *et al*, "Simplex-coded BOTDA fiber sensor with 1 m spatial resolution over a 50 km range," Opt. Lett. **35**(2), 259-261 (2010).
[7] F. Rodriguez-Barrios, *et al*, "Distributed Brillouin Fiber Sensor Assisted by First-Order Raman Amplification," J. Lightwave Technol. **28**(15), 2162-2172 (2010).
[8] M. A. Soto, *et al*, "Extending the real remoteness of long-range Brillouin optical time-domain fiber analyzers," J. Lightwave Technol. **32**(1), 152–162 (2014).
[9] M. A. Soto, G. Bolognini, and F. Di Pasquale, "Simplex-Coded BOTDA Sensor Over 120 km SMF with 1 m Spatial Resolution Assisted by Optimized Bidirectional Raman Amplification," IEEE Photon. Technol. Lett. **24**(20), 1823-1826 (2012).
[10] M. A. Soto, J. A. Ramírez, and L. Thévenaz, "Intensifying the response of distributed optical fibre sensors using 2D and 3D image restoration," Nat. Commun. **7**, 10870 (2016).
[11]. M. A. Soto, *et al*, "Intensifying Brillouin distributed fibre sensors using image processing," Proc. SPIE **9634**, 96342D (2015).
[12] A. Buades, B. Coll, J. M. Morel, "A review of image denoising methods, with a new one," Multiscale Model. Simul. **4**(2), 490–530 (2005).